Geothermics 102 (2022) 102378

Contents lists available at ScienceDirect

Geothermics

journal homepage: www.elsevier.com/locate/geothermics

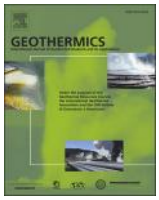

Occurrence, origin and health risk of arsenic in water and palm dates from the Bazman geothermal field, SE Iran

Adnan Deshaee [a], Ata Shakeri [a,b,*], Behzad Mehrabi [a], Meisam Rastegari Mehr [a,b], Seyed Kazem Ghoreyshinia [a]

[a] Department of Applied Geology, Faculty of Earth Science, Kharazmi University, Tehran 15614, Iran
[b] Water Research Center, Kharazmi University, Tehran 15614, Iran

ARTICLE INFO

Keywords:
Bazman Field
Hyderogeochemical Processes
Arsenic
Health Risk Assessment
Springs
Heavy metals

ABSTRACT

Investigating drinking and irrigation water quality in areas with water crises such as Southeastern Iran is vital. Hyderogeochemical processes, the origin and fate of arsenic were studied in the Bazman geothermal area. For this purpose, thermal springs, surface and groundwater, and surrounding rocks were sampled and the samples analyzed (main ions, trace elements and stable isotopes). Several samples were also collected from date palms irrigated by this water for As, Cu, Ni and Zn analysis and the associated health risk indices calculated. In general, Bazman springs have a neutral to slightly alkaline pH, is of a predominant Na-Cl water type, and the hydrochemistry of the springs' water is affected by water-rock interaction, silicate weathering, dissolution and evaporation. The ion exchange diagrams also indicate the influence of cation exchange on the water chemistry in the region. Geochemical and statistical analysis showed that the origin of arsenic and other trace elements in the aquifer is water-rock interaction. It seems that during water ascent to the surface As is transported by arseno–carbonate complexes in the Bazman geothermal aquifer. In addition to carbonates, iron-rich minerals such as goethite and hematite also influence the concentration of dissolved arsenic in the spring's water. Arsenic concentration in sediments and outcropped rocks adjacent to the springs showed that high levels of arsenic concentration in spring water cannot be related to these rocks and sediments. A recorded high target hazard quotient (THQ) value of arsenic in date samples alarmed the possible adverse health effects for the consumers. Also, hazard index values are higher than unity, invoking a concern for public health.

1. Introduction

In many regions, volcanic and geothermal activity is believed to be one of the causes of high arsenic and other environmental contaminant such as fluoride (F), boron (B) and antimony (Sb) concentrations in ground and surface waters (Kaasalainen and Stefánsson, 2012; Shah et al., 2015; Webster and Nordstrom, 2003). Arsenic, notoriously known as a toxic and carcinogenic metalloid, is a ubiquitous trace component in geothermal systems (Feng et al., 2014; Keller et al., 2014; Maizel et al., 2016; Mohammadi et al., 2021). The presence of As and other toxic elements in geothermal waters and related environmental impacts have long been recognized in many countries of the world, e.g., USA (Wilkie and Hering, 1998); Mexico (Birkle and Merkel, 2000; González et al., 2001); Iran (Mosaferi et al., 2003; Shakeri et al., 2015) and Latin America (López et al., 2012). High concentrations of As have also been found in mature Na-Cl waters that have been in contact with As-bearing rocks for a long period of time (Birkle et al., 2010), suggesting that the increase in As concentration is due to the longer residence time (elemental leaching) of the waters.

Natural contamination of groundwater with metals and metalloids due to the mixing of cold waters with geothermal fluids is often associated with a high total dissolved solids content and significant concentrations of As, B, F and other trace elements (Smedley and Kinniburgh, 2002; Brown and Simmons, 2003; Angelone et al., 2009; Landrum et al., 2009; Aksoy et al., 2009; Henke, 2009). Thermal waters are used for human recreational and health purposes i.e., treatment of skin diseases, sciatica, rheumatism, lumbago, general tiredness and nervous associated disorders. Many studies have highlighted an increased risk of skin, lung and bladder cancers, as well as a range of non-cancer diseases among populations drinking water with elevated levels of arsenic (Hopenhayn-Rich et al., 1996, 1998; Smith et al., 1998; Tseng et al., 2003).The release of these waters into the surrounding

* Corresponding author.
E-mail address: atashakeri@khu.ac.ir (A. Shakeri).

https://doi.org/10.1016/j.geothermics.2022.102378
Received 7 October 2021; Received in revised form 5 February 2022; Accepted 12 February 2022
Available online 31 March 2022

environment may not only raise concern about the aquatic ecology (Mroczek, 2005), but could also pose a health risk to local residents when it used for drinking or irrigation purposes (Robinson et al., 2003; Komatina, 2004; Agusa et al., 2006).

Human exposure to arsenic (As) at toxic levels has been reported in some areas of Iran, particularly during the last two decades (Sheikhi et al., 2021; Alidadi et al., 2019; Mosaferi et al., 2003). However, in most cases; especially in the geothermal areas; only limited data are available on the sources and occurrence of As, making a correct assessment of the scale and magnitude of this problem difficult (Shakeri et al., 2015; Sharifi et al., 2016, 2020; Ghoreyshinia et al., 2020; Rastegari Mehr et al., 2020) but crucial for confronting such health and environmental impacts.

The Bazman geothermal field is located in the southwest of Iran. Economically the rural area of the Bazman is one of the poorest regions in the country; the climate is arid and water is concurrently scarce with a poor quality of the limited water resources i.e., high salinity and geogenic pollution are major concerns for access to safe drinking water. Due to the lack of safe and clean water resources, many cold and thermal springs are the main sources of water for sanitary consumption and agricultural purposes in the rural area. The main objectives of this study are: 1) to investigate hydrochemical status of springs and river water in Bazman area, 2) to determine arsenic contamination, sources and fate, and 3) to assess the health risk of local residents' exposure to As through consumption of date palm irrigated by surface waters.

2. Materials and methods

2.1. Study area

The Bazman geothermal field lies within the Makran structural zone in southeastern Iran, between 27° 36' N - 27° 52' N latitudes and 59° 57' - 60° 11' E longitudes (Fig. 1). The Late Miocene-Pleistocene Bazman stratovolcano (3490 m.a.s.l.) is composed primarily of andesitic to dacitic lava flows and pyroclastic rocks of 7.5 Ma (Pang et al., 2014) to 0.7 Ma (Conrad et al., 1981) radiometric age. A number of small andesitic lava flows and peripheral basaltic cinder cones have also been discovered in the region (Saadat and Stern, 2011; Conrad et al., 1981). The study area is bounded by the Palaeozoic sedimentary rocks that have experienced contact metamorphism locally and shale, sandstone, limestone and dolomite as the most common sedimentary rocks. The sedimentary country rocks have metamorphosed to hornfels, quartzite and marble depending on the local lithology near their interaction with the main Bazman Granitoid Complex (Vahdati Daneshmand et al., 2004; Sahandi and Padashi, 2005) (Fig. 1). The spring water samples of the Bazman geothermal field collected at 27 to 54 kilometer distances south of the Holocene Bazman cone. Based on Deshaee et al., 2020, these springs are divided into four groups based on their locations (Fig. 1 and Table 1). These four groups include: A) Sargar, cold spring, Hamam Bazman 1 and, 2 springs (samples B1, B2, B10 and B13); B) Koozeh 1, Koozeh 2 and Khaneh Gel springs and Surface water (samples B3, B4, B7 and B11); C) Abgarm Bazman 1 and 2 springs (samples B5 and B6); and D) Espidezh, Maksan 1 and Maksan 2 springs (samples B8, B9 and B12). The springs' discharge rates ranged from less than 1.5 L/s (Abgarm Bazman 1) to more than 50 L/s (Koozeh 2), with water temperatures ranging from 27 °C to 44 °C (Deshaee et al., 2020). The nearest urban area in the study area is Bazman City, with a populations more than 5190. Also, more than 40 villages are located near the Bazman volcano that are directly or indirectly affected by its associated geochemical processes and impacts. June and August are the hottest months in the area, with a mean maximum temperature of 32 °Celsius. The average annual rainfall in the area is only 112 mm.

2.2. Sampling and analysis

A total of 11 thermal spring water samples, a surface water sample and a cold spring sample were collected in August 2017. (Fig. 1). Physicochemical parameters such as pH, Eh, TDS, and electrical conductivity (EC) were measured on site using a calibrated portable HACH multimeter. All water samples were filtered using 0.45 μm membranes and stored in 350 mL polyethylene bottles that had been rinsed twice with deionized water. For cations and trace element analysis, reagent-grade HNO_3 with a molar concentration of 14 M was added to each sample for bringing the pH below 2. Silica (after dilution using deionized

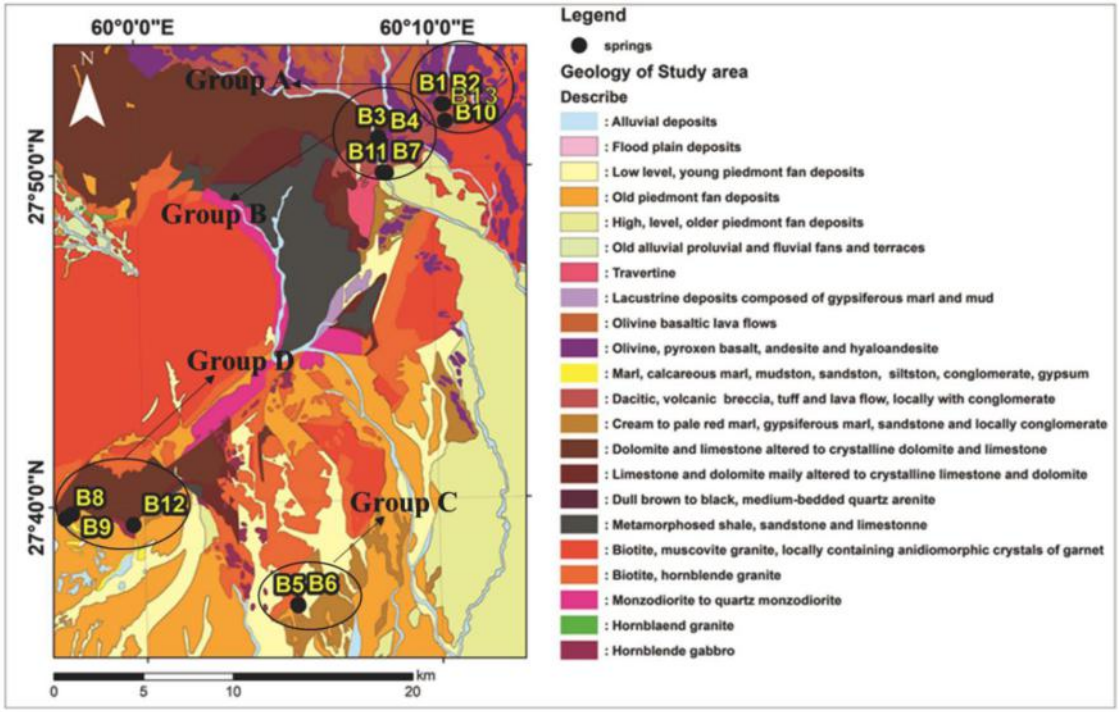

Fig. 1. Geological map of the study area and sample locations (base map modified after Vahdati Daneshmand et al., 2004; Sahandi and Padashi, 2005).

Table 1
Field measurements, chemical and isotopic composition of water samples. δ_D and $\delta^{18}O$ is relative to V-SMOW, star cell means no data.

Group	A	A	B	B	C	C	B	D	D	A	B	D	A
ID	B1	B2	B3	B4	B5	B6	B7	B8	B9	B10	B11	B12	B13
T °C	37.1	35.3	37.7	34.3	44	41	28.1	35.5	34.5	27	33.0	34.5	21
pH	7.2	7.1	7	6.8	7.9	8.4	7.6	7.1	7.4	7.4	7	7.2	8.5
EC (μS/cm)	1032	1070	2063	2639	10,583	11,024	3087	1455	1329	2171	2536	1375	1685
TDS (mg/L)	813	778	1707	1304	6848	6917	2180	846	1078	1467	1379	793	1258
Eh (mV)	74.5	75	17.8	16.2	92.9	95.2	63	26	25.5	16.7	15.8	25.4	67
Major components (mg/L)													
HCO_3	122	117	397	370	52	45	458	260	305	299	384	241	295
Cl	204	189	417	440	3337	3532	639	220	201	366	462	195	347
SO_4	120	124	180	103	384	384	230	124	132	264	150	124	278
Ca	27	29	98	100	662	645	139	58	55	97	95	46	65
Mg	4.4	4.3	27	29	40	30	45	20	20	8.3	32	28	21
Na	155	161	277	285	1450	1460	356	178	175	310	283	153	361
K	11	10	17	18	30	30	38	4.3	4.4	15	18	5.3	15
SiO_2	83	83	44	40	39	41	51	21	20	89	35	22	88
B	8	6.2	7.7	7.3	17	20	7.5	7.2	6.7	6.3	7.5	6.2	7.9
F	0.5	0.4	*	*	0.7	0.7	*	*	0.4	0.4	*	*	0.6
Trace elements (μg/L)													
As	21.4	19.8	75.3	83.4	36	29.5	123.2	25.6	26.8	29.9	70.8	10.6	82.2
V	118	116	38.1	36.7	5	2	22.3	12.3	12.2	178	35.7	3.8	95.3
Mo	8.3	9	3.5	2.7	49.5	48.2	8.9	7	11.2	14.6	3	8.4	17.3
Se	11.1	11.7	5.2	5.5	93.2	87.2	2	5.9	5.6	7.1	5.7	0.1	13.8
Cr	3.1	4.1	9.4	18.6	37.2	36.7	3.6	8.6	44	2	24.2	3	6.9
Al	150	90	40	40	180	180	10	50	30	40	30	40	260
Fe	70	50	1	40	40	60	3	1	70	60	100	8	30
$\delta^{18}O$	−3.7	−3.1	−1.9	*	−2.3	−2.9	−2.4	*	*	*	*	*	*
δ_D	−24.9	−23.4	−19.6	*	−22.2	−21.9	−15.3	*	*	*	*	*	*

water to prevent the precipitation of SiO_2), cations and other trace elements were analyzed by ICP-OES/MS methods at Zar-Azma Lab., Tehran, Iran. Bicarbonate was measured in laboratory using standard titration method, whereas SO_4 and Cl concentrations were analyzed for by ion chromatography (IC). The ionic balance of the samples is in the range of 0.91% to 7.56% with an average of 3.87%. The uncertainties are ±5% for ICP-MS and IC, respectively. Isotope analysis of water samples was carried out using a Finnigan MAT Delta plus XP and Gas Bench at the University of Ottawa, Canada. For this study five rock samples adjacent to the springs were collected (B3, B4, B5 and two samples from B8) and shipped to the laboratory for elemental analysis. Rock samples were powdered and homogenized down to less than 63 μm size. The powdered samples were dissolved in 5 ml aqua regia + 1 ml HF using a CEM (MDS-2000) microwave digestion oven at 7 atm for 30 min. The total concentrations of arsenic and other selected trace elements were determined using ICP-MS at Zar-Azma Lab. Tehran, Iran.

Four date composite samples which were irrigated with some of these water samples (B3, B8, B10 and B13) were collected for analyzing selected trace elements. Dates washed with deionized water several times to remove all external contaminants, oven-dried at 70 °C until reaching a stable weight and analyzed for selected trace elements (As, Cu, Ni and Zn) after digestion with concentrated hydrochloric acid using ICP-MS (at Zar-Azma Lab). Duplicate analyses, procedural blanks, and appropriate reference materials (STD CDV-1 and STD OREAS45EA) were used for evaluating the quality assurance and quality control (QA/QC) of the analytical data. The relative standard deviation (RSD) was less than 6% for each element, and the recovery percentages ranged from 94 to 102%, 97 to 104%, and 92 to 105% for water, rock and date palm samples, respectively, and the blanks were below the detection limit.

2.3. Daily intake of metals

The following method was used to determine the daily intake of metals (DIM) in the study area.

DIM = C metal*C factor*D intake / B average weight

Where C metal, C factor, D intake and B average weight represent the trace elements' concentrations in plants (mg / kg), conversion factor, daily intake of date and average body weight, respectively. The conversion factor of 0.085 was used to convert fresh date weight to dry weight, as described by Waheed et al. (2005). The average daily date intakes for adults in the study area was considered to be 68 g / person day (Karizaki, 2017), while the average adult body weights were considered 70 kg, as used in a previous study in Iran (Shakeri et al., 2020).

2.4. Target hazard quotient (THQ)

Target hazard quotients (THQ) are used to evaluate the non-carcinogenic risk of toxic elements on human by date consumption. When the THQ for a certain pollutant is below unity, there is no risk for the particular endpoint; whereas THQ greater than unity shows a greater level of concern for exposed populations. The THQ is calculated using Eq. 6 (USEPA, 2011):

THQ = (DIM * EF * ED) / (RfD * BW * ATn)

Where, THQ is the target hazard quotient, DIM the daily intake of metals, EF the exposure frequency (365 days/year), ED the exposure duration (years) over lifetime (70 years) for non-carcinogens as per assumptions (USEPA, 2011). RfD the reference dose of an individual metal (mg/kg/day) (As = 0.0003, Cr = 0.003, Cu = 0.04, Ni = 0.02, Pb = 0.036 and Zn = 0.3) (USEPA, 2011), BW an average adult body weight (70 kg), ATn the average exposure time for non-carcinogens, 25,550 days or 70 years (Shakeri et al., 2020).

The hazard index (HI) evaluate the potential risk to human health through more than one trace element (Song et al., 2015). HI is calculated using Equation (7):

$HI = \sum THQ$

When, an index value < 1 is assumed to be safe over a lifetime.

3. Results and discussion

3.1. Physicochemical and hydrogeochemical characteristics

The physicochemical parameters and major ion concentrations along with selected toxic and trace element concentrations of the thermal spring waters in the Bazman geothermal area are presented in Table 1. As shown in Table 1, the thermal waters have temperature range of 27 to 44 °C, and a pH value range of 6.8 to 8.5 indicating a weak alkalinity. The TDS values of the thermal water samples are between 775.5 to 6917 mg/L, indicating lower concentrations than that of the drinking water standard, except for B3, B5, B6 and B7 thermal spring waters. Main cations include Na and Ca, occurring at concentration ranges of 153.4–1460 mg/L and 27.3– 662 mg/L, respectively. Main anions include Cl and HCO_3 (except in B5 and B6 spring waters), ranging from 188.6 to 3532.2 mg/L and 21.3 to 457.5 mg/L, and proportions of 29.8 to 57.64% and 0.34 to 24.02%, respectively. The B5 and B6 spring waters have the lowest concentration of HCO_3 among the samples. A Piper diagram (Supplementary material 1-S1) illustrates the dominant hydrochemical features of geothermal waters in the study area. According to the Piper diagram Na and Cl are the dominant cations and anions in all water samples, respectively and the water is of the Na-Cl type. The water samples on the Piper diagram plot in various fields with respect to other main ions and each group has a specific sub-type. Overall, the samples of each group (groups A, B, C and D) have a similar origin and the small changes in each group show effects of hydrogeochmical processes, probably due to waters ascending to surface, mixing with groundwater evaporating or dissolving.

The Gibbs (1970) diagram is widely used in many regions to identify the major factors controlling groundwater chemistry (Adimalla and Venkatayogi, 2018; Narsimha and Sudarshan, 2017; Koffi et al., 2017; Li et al., 2016).) Fig. 2. reveals that the groundwater samples plot between the rock weathering and evaporation dominant fields, which suggests that the chemistry of the groundwater is influenced by rock weathering, water–rock interaction, evaporation and dissolution. Isotope studies ($\delta^{34}S$) of some of the Bazman thermal springs by Deshaee et al., 2020 indicated the influence of gypsum and anhydrite dissolution from the host rock on water chemistry.

Bivariate mixing plots of Na-normalized Mg vs. Na-normalized Ca and Na-normalized HCO_3^-vs. Na-normalized Ca, examine the relative contribution of the main three processes including silicate weathering, carbonate and evaporite dissolution and solute concentration in groundwater (Gaillardet et al., 1999; Mukherjee and Fryar., 2008; Mukherjee et al., 2012). Dominance of bicarbonate and sulfate ions rather than those of calcium and magnesium reveal the superiority of silicate weathering (Elango et al., 2003). Silicate weathering and evaporite dissolution are recognized as the main processes controlling the groundwater solute concentration (Supplementary material 2-S2). Low concentrations of Mg^{2+} and Ca^{2+} in samples, could be the consequence of secondary mineral formation in the low-temperature geothermal system (Ellis, 1971). At a normal geothermal gradient, hydrolysis processes decrease the reactivity of magnesium, whereby the magnesium concentration in groundwater increases. Furthermore, in geothermal systems with a low salinity, Mg^{2+} concentrations and Mg/Ca ratios are extremely low; these characteristics are common in geothermal systems since Mg^{2+} and Ca^{2+} are retained in the solid phase when secondary minerals such as micas, kaolinite, montmorillonite, chlorite, illite are formed (Ellis, 1971; Bischoff and Seyfried, 1978). The plot of HCO_3^- vs. Ca (Supplementary material 2-S2) suggests that silicate weathering may be the main source of ions in water samples (except group C). Samples from group C plot in the evaporite dissolution dominant field, maybe because this group plots in the partially mature field (Deshaee et al., 2020) or the dissolution of anhydrite and gypsum has affected the water chemistry. In general, the composition of these waters depends on the host rocks and the mixing rate at shallow levels with ground waters (Deshaee et al., 2020).

Geochemical weathering is basically governed by the nature of the host rock, the rate of weathering and climate conditions (Mukherjee et al., 2009) Tardy (1971). suggested that most of the ions in water from granitic terrains originated from the weathering of K-feldspar, plagioclase and biotite, where cations (e.g., K^+, Na^+ and Ca^{2+}) were released by breakdown of minerals and ended up in solution, Al_2O_3 was released by the breakdown of these minerals remained fixed in secondary minerals whereas SiO_2 was released by both processes. Geologically, the study region is occupied by granite, gneissic and evaporite rocks. According to Garrels (1967), water composition from granitic rocks plots in the kaolinite stability field while the water composition from basic rocks remains in the montmorillonite stability field.

Activity diagrams were used to estimate the mineral alteration and fluid mineral equilibrium, caused by the water–rock interaction in the

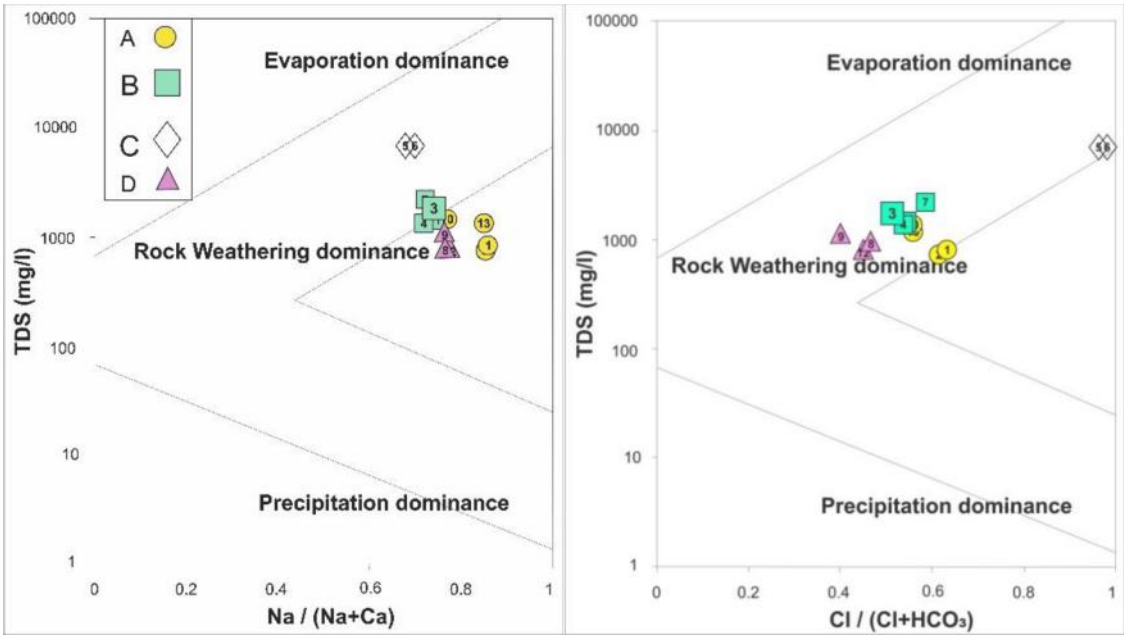

Fig. 2. TDS vs. Na/(Na+Ca) (a) and TDS vs. Cl/(Cl+HCO_3) (b) plots showing the dominant mechanisms controlling the water chemistry.

aquifer. Illustrations of phase relations were evaluated in these diagrams constructed by Tardy (1971). The silicate equilibrium condition for the Bazman water samples were examined by Na^+–H^+–SiO_2, K^+–H^+–SiO_2 and Ca^{2+}–H^+–SiO_2 mineral balance diagrams (Fig. 3a. b and c). The results show that the Bazman water samples fit in the kaolinite and Na-Montmorillonite (Fig. 3a), K-feldspar and kaolinite (Fig. 3b) and kaolinite (Fig. 3c) stability fields, indicating effects of andesitic rock forming minerals weathering. In the study area, K-feldspar, quartz, plagioclase, mica and amphibole are major minerals and due to water-rock interaction, these silicates have been weathered and Na-feldspars altered to kaolinite. Reactions of some silicates (plagioclases, K-feldspars) have an incongruent dissolution and may form montmorillonite and kaolinite (Loughnan, 1969; Drever, 1988). Na^+ and HCO_3^- concentrations in some hydrothermal waters are also controlled by exchange process rates with silicates in rocks altered to clays (Fig. 3; Gemici and Tarcan, 2002) Fig 3.a shows that group A and C spring waters plot in the Na-Montmorillonite field and others plot close to the line between Na-montmorillonite and kaolinite, indicating the effect of cation exchange on the Bazman water chemistry. Saturation indices of various minerals calculated by the PHREEQC hydrogeochemical code (Parkhurst and Appelo, 1999) shows that all the water samples are over-saturated with respect to kaolinite. The results for mineral balance diagrams are in agreement with the calculation of saturation indices (SI) for kaolinite and all groundwater samples are over-saturated with respect to kaolinite.

Multivariate composition graphs were used for evaluating ion exchange and reverse ion exchange processes in the spring waters (Supplementary material 3-S3). Na/Cl vs. EC bivariate plots for the thermal spring waters, shows that almost in all samples (except group C and B7) the Na/Cl ratios are higher than 1, suggesting that although the fluid salinity could be related to the halite dissolution, but the ion-exchange process impacts the water chemistry (Srinivasamoorthy et al., 2008). Based on the Ca + Mg vs. HCO_3 + SO_4 bivariate plot line 1:1 represents the calcite, dolomite, and gypsum dissolution. Whereas, samples that plot above and below of the line 1:1 are affected by reverse ion exchange and ion-exchange processes, respectively (Kalantary et al., 2007; Zaidi et al., 2015). A weak relationship between alkaline earths (Ca+Mg) and HCO_3+SO_4 provides an additional evidence for an ion-exchange process in the Bazman waters. When HCO_3+SO_4 values are lower than 5 meq/L and the samples fit the 1:1 line, dissolution of calcite and dolomite is the significant process that affects the water chemistry (Kalantary et al., 2007). The samples from the Bazman springs (except group C) lie under the 1:1 line in Ca + Mg vs. SO_4 + HCO_3 diagram and HCO_3+SO_4 values for all samples are higher than 5 meq/L, indicating a simultaneous ion exchange. These findings are also confirmed by the TDS vs. (Na- K)/ (Na-K+Ca) diagram, in which a tendency toward 1 for (Na-K) / (Na-K+Ca) with increasing TDS observed in most water samples from the Bazman springs, except those in group C. The different features of group C springs, have been previously discussed by Deshaee et al. (2020), where a deep aquifer associated with evaporitic lenses is in contact with a young cooling plutonic body, while groundwater mixed with hydrothermal waters was considered as the main origin of the other spring water groups.

Mineral equilibrium calculations are useful in predicting the presence of reactive minerals and estimating mineral reactivity in a groundwater system (Deutsch, 1997). Mineral saturation indices (SIs) for possible hydrothermal minerals in the geothermal system reservoir were calculated at the outlet temperature and measured pH using the PHREEQC computer code (Parkhurst and Appelo, 1999).

Results of SI calculations for the Bazman thermal springs are presented in Supplementary material 4-S4. The waters are supersaturated with respect to goethite, hematite, kaolinite and quartz and unsaturated with alunite, anhydrite, arsenolite, As_2O_5, gypsum, halite and siderite. Also, in the Bazman geothermal area 30.76%, 38.46 and 7.69% of the

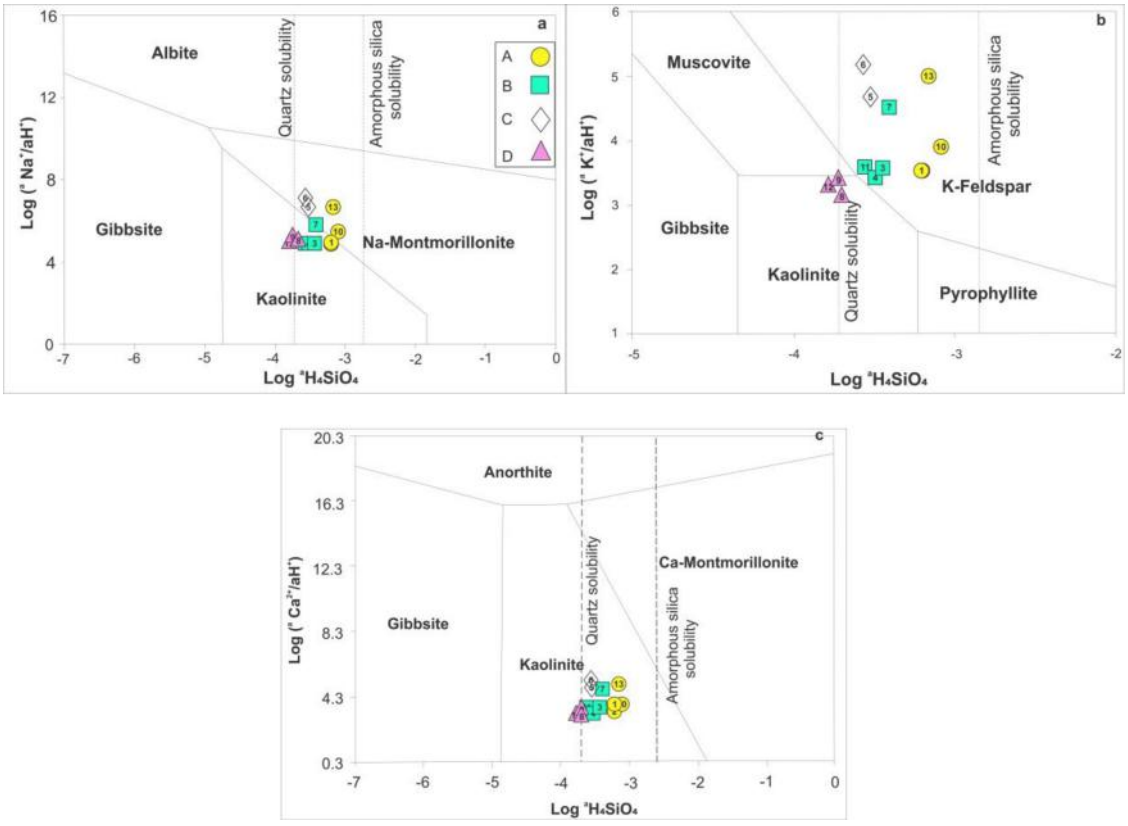

Fig. 3. Stability field diagrams(based on the actual temperatures of the springs) for the Na^+-H^+-SiO_2 (a), K^+-H^+-SiO_2 (b) and Ca^{2+}-H^+-SiO_2 (c) systems in Bazman aquifer.

groundwater samples are unsaturated with respects to calcite, dolomite and Fe $(OH)_3$(a), respectively.

3.2. Arsenic geochemistry

Geochemical data shows that the As concentrations are in the range 10.6–123.2 μg/L (Table 1) indicating higher concentrations than the WHO provisional guideline value for arsenic of 10 μg/L (WHO, 2011). The highest arsenic concentration is recorded in water sample B7 (a drainage outflow from springs Koozeh 1 and Koozeh 2) which probably suggests that at least some of the arsenic accumulation is related to near-surface evaporation. The hottest spring waters of group C (including those with temperatures between 41 and 44 °C) have comparatively low arsenic concentrations. The concentrations of As in the water samples have been plotted against B, Na, Cl, HCO_3, K and F values (Supplementary material 5-S5).

Group C spring data were removed due to their high dissolved element concentrations in diagrams S5 (a, b, c and f). These spring waters (Group C) have the highest values of Na, F, B and Cl, and during data normalization and statistical analyses, this ruins the correlation of the data, therefore, for evaluating the relationship between arsenic and other elements, group C data is excluded. However, as mentioned in our previous work (Deshaee et al., 2020), the springs of group C are very different in terms of origin and geochemistry from the other spring groups. Arsenic shows a positive correlation with Na, F, B and Cl.

A relationship between arsenic and boron in groundwater has also been reported by other investigators (Smedley et al., 2002; Bhattacharya et al., 2006). The correlation of arsenic with boron and fluorine concentrations (except group C, which does not show any correlation) may indicate a common origin for these elements. A positive correlation between bicarbonate and arsenic (S6-d) indicates that this ion can play an important role in the mobilization of arsenic through the competition for adsorption sites and by the formation of arseno–carbonate complexes (Kim et al., 2003; Bhattacharya et al., 2006). The relatively good correlation of potassium with arsenic concentrations as well as bicarbonate and sodium concentrations (S6-b, d and e) could be the possible result of a hydrochemical process such as hydrolysis of K-feldspars and albite, which can lead to an increase in K, Na, and HCO_3 concentrations of water.

According to Supplementary materials 5 and 6 (S5, S6), it may inferred that the origin of arsenic and other elements is from the water-rock interactions in the deep aquifer and during ascent to the surface. Arsenic levels in groundwater are also controlled by carbonates by forming complexes with arsenic, which means that the higher the concentration of carbonate in the water leads to a further mobility of arsenic (Bhattacharya et al., 2006). In addition to carbonates, iron minerals such as goethite and hematite also control the concentration of soluble arsenic. In general, arsenic and arsenic-bearing minerals can adsorb up to 76,000 mg / kg of iron oxides and hydroxides (Pal et al., 2002; Smedley and Kinniburgh, 2002). By looking at the As correlation diagram (S6) with hematite and goethite, which is constructed by the PHREEQC software, it is obvious that, when goethite and hematite are supersaturated, the arsenic concentration decreases in the water.

Due to high As concentrations in the water samples, it is crucial to examine the relationship between evaporation and As concentrations in the waters studied. High evaporation rates could increase pH and salinity in the water, in turn facilitating a desorption reaction of As from mineral oxide surfaces (Mladenov et al., 2014; Camacho et al., 2011; Nickson et al., 2005). Small oxygen and hydrogen isotopic shifts in the $\delta^{18}O$ and δ_D plot caused by surface evaporation or both evaporation and water-rock isotopic exchange, which have been discussed in our previous work (Deshaee et al., 2020) Fig. 4. shows a positive trend between $\delta^{18}O$ and As concentration ($r^2 = 0.68$). As-rich waters show an increase in heavy $\delta^{18}O$ values, indicating the contribution of meteoric recharge and evaporation. These processes might be contributing towards As enrichment in groundwater to some extent.

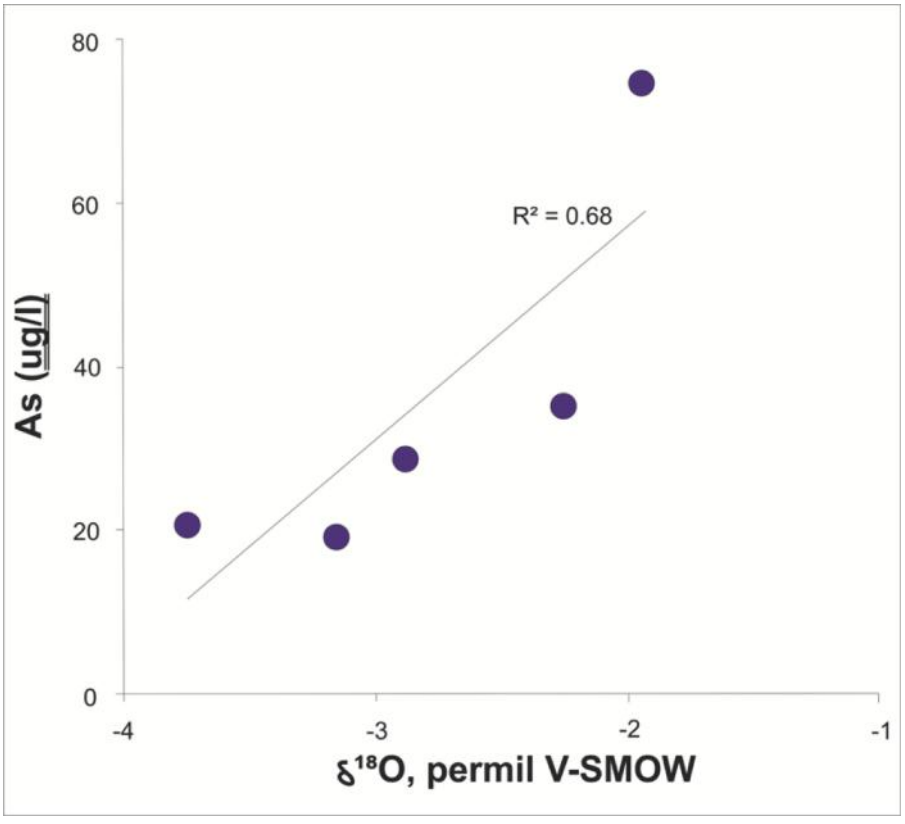

Fig. 4. Relationship between arsenic and $\delta^{18}O$.

Groundwater at all sites studied is highly under-saturated with major As phases (e.g. arsenolite and As_2O_5), indicating that As should generally remain dissolved in the water after mobilization. Redox potential (Eh) and pH are the most important factors that control the predominant form or speciation of the arsenic in the water environment. Under oxidizing conditions, $H_2AsO_4^-$ is dominant at low pH (less than 6.9), whilst at higher pH, $HAsO_4^{2-}$ becomes the dominant species. In the neutral and slightly alkaline waters, As^{III} species are dominant and the major species are $HAsO_2$ and $As(OH)_3$ (Planer-Friedrich et al., 2007). According to previous studies in numerous geothermal areas worldwide, H_3AsO_3 is the predominant species at depth and during ascent, reduced species of arsenic, oxidize to H_3AsO_4 (Schwenzer et al., 2001; Webster and Nordstrom, 2003). Supplementary material 7 (S7) shows the dominance of As^V in Bazman water samples and all of the specimen fit into the $HAsO_4^{2-}$ dominance field. Assuming thermodynamic equilibria prevail, As released into an oxygenated surface water as H_3AsO_3 should undergo immediate oxidation to arsenate ions: H_2AsO_4 at $\leq$ pH 6.9, $\geq$ $HAsO_4^{2-}$ (Aggett and Aspell, 1978; Nimick et al., 1998).

3.3. Arsenic concentration in rocks and sediments

To investigate the arsenic concentration in the alluvial sediments which covered the study area, and the possible relevance with water, data for 49 sediment samples were obtained from Iran's Geological Survey. The arsenic mean concentration in sediments is 8.6 mg/kg, and the lowest and highest values are 1.3 and 14.4 mg/kg, respectively (Supplementary material 8-S8). These values are close to average As values reported elsewhere for similar sediments (Shamsudduha et al., 2008; Smedley and Kinniburgh, 2002). The arsenic level in sediments near the springs is low, therefore the high arsenic concentration in the water couldn't be interrelated to alluvial sediments.

Arsenic concentrations in surrounding rocks of the Bazman geothermal area are presented in Table 2. Five samples around the study area from groups B (B3 and B4), C (B5) and D (two samples from B8) were analysed for the composition of these rocks (arsenic concentration and other trace elements). The results showed that these rocks have a low arsenic concentration. The highest arsenic concentration in rock samples was related to group D (the arsenic concentration in a limestone sample was below the detection limit) and C spring waters had concentrations of 3.1 and 2.3 mg/kg, respectively. These values are close to the average As concentration, and indicate that the high arsenic concentration of the spring waters is not related to that of the surrounding rocks. The mode of this distribution is in the class of 0–10 mg/kg, more or less similar to the ranges (0.2–15 mg/kg) quoted by other authors for world-wide granitic rocks (Boyle and Jonasson, 1973; Rose et al., 1979; Rielel and Eikman, 1986). Low As concentrations in sediments and surrounding rocks indicate that the sources of arsenic in the Bazman waters were triggered by the specific hydrogeochemical conditions of the flow path in the Bazman granitoid complex.

3.4. Arsenic and other trace element health risk assessment

Currently the Bazman springs are mainly used by local inhabitants for external use (e.g., bathing), which is thought to be the least hazardous arsenic contamination pathway (Zartarian et al., 2006). However, changing agricultural practices in the area e.g., irrigation of date palms by using this water could lead to a possible arsenic passage into the human food chain with possibly more hazardous consequences. The arsenic concentration in a cold spring (B13 sample) was 82.2 μg/L, which corresponds to about 8 times that of the WHO standard (10 μg/L). Such high levels of As are extremely toxic in drinking waters. Therefore, the high level of the toxic element demonstrates a potential health risk to the inhabitants of the study area. The arsenic chemistry in the waters of Bazman area seems to be controlled primarily by the reservoir rock geochemistry. As a natural outcome of this situation, arsenic levels in cold surface and thermal waters are also above the WHO standard limits.

The recorded high level of measured arsenic and other trace elements and ions may affect the plants of the area because all these water samples are used for irrigation purpose (e.g. date palms).

Date samples collected from the study area, exhibited the following average of trace element concentrations; As—28 μg/kg; Cu—1750 μg/kg; Ni—110 μg/kg; and Zn—2290 μg/kg. The mean concentration for the daily intake of As, Cu, Ni and Zn in the area is 0.015, 0.95, 0.062 and 1.25 μg/kg, respectively. Non-carcinogenic effects of toxic elements were assessed using a target hazard quotient (THQ) and a hazard index (HI) (Table 3). THQ values of Cu, Ni and Zn over the whole study area are far below 1, while, As had the highest THQ value. The high THQ value of arsenic in samples B3 and B8 is 0.8 and 1.1, respectively, suggesting possible adverse health effects for consumers in area B8. Also, HI values in all samples are higher than unity (except B3), indicating a concern for public health. This hazard is mainly relevant to arsenic contamination in date palms irrigated with high As water. According to previous observations in the world (Zhang et al., 2012; Rodríguez-Lado et al., 2013; Giménez-Forcada and Smedley, 2014) we could confirm that the observed As concentrations pose a health threat, and thus implications for water management policy and health are needed to reduce possible environmental and public health risks.

4. Conclusions

In this study, possible hydrogeochemical processes in spring, surface and groundwaters of the Bazman geothermal area, along with arsenic and trace element behavior in water, rock, sediments and palm date were examined. The concentrations of the main ions in the Bazman spring waters including Na^+ and Cl^-, ranged from 153.4 to 1460 mg/L and 188.6 to 3532.2 mg/L, respectively, with a neutral to slightly alkaline pH (ranges from 6.8 to 8.5). The findings revealed that ion exchange, water-rock interaction, silicate weathering, dissolution, and evaporation all influence the water chemistry of these springs. High arsenic concentrations (10.6–123.2 μg/L), are possibly due to water-rock interactions, by which arseno–carbonate complexes may form in the ascending water. However, based on the saturation index, the presence goethite and hematite which are rich in As, also may control the concentration of dissolved arsenic in springs. Nearby alluvial sediments and rocks adjacent to the spring waters (with mean As concentrations of 8.6 mg/kg and 2.1 mg/kg, respectively) did not have any impact on the water chemistry especially not the arsenic concentration. Considering a high hazard quotient value (1.09) for As in date palm samples, the irrigation of the plants by a high arsenic concentration water, poses a health risk to inhabitants and consumers, suggesting a rigorous water management policy and proper monitoring and control for reducing environmental impacts and public health risks. Due to the

Table 2
Trace elements concentrations in surrounding rocks of Bazman's springs.

Element	Unit	Min.	Max.	Mean
As	mg/kg	1.3	3.1	2.1
Cr	mg/kg	1	31	14.8
Mo	mg/kg	0.3	1.2	0.9
Se	mg/kg	1.7	2.5	2.1
U	mg/kg	0.1	4.8	2

Table 3
Target hazard quotient (THQ) and hazard index (HI) of As, Cu, Ni and Zn.

Sample. no	THQ				HI
	As	Cu	Ni	Zn	
B03	0.809	0.391	0.037	0.067	1.304
B08	1.096	0.391	0.035	0.063	1.584
B10	0.365	0.196	0.019	0.048	0.628
B13	0.678	0.391	0.088	0.061	1.220

fact that irrigation of arable lands with arsenic-contaminated water can lead to a further soil contamination, and the soil environment mediates the transfer of elements from irrigation water to the crops, a geochemical study of arsenic and other trace elements in soil and the relationship of physicochemical parameters on its transfer and bioavailability may be helpful for planning a viable water resource management, crop quality and regional public health.

CRediT authorship contribution statement

Adnan Deshaee: Writing – original draft, Software. **Ata Shakeri:** Data curation, Conceptualization, Resources, Supervision. **Behzad Mehrabi:** Validation, Writing – review & editing, Investigation. **Meisam Rastegari Mehr:** Formal analysis, Writing – review & editing. **Seyed Kazem Ghoreyshinia:** Writing – original draft, Software.

Declaration of Competing Interest

The authors declare that they have no known competing financial interests or personal relationships that could have appeared to influence the work reported in this paper.

Acknowledgments

The authors wish to express their gratitude to Kharazmi University and water research center of the University for logistic supports.

Supplementary materials

Supplementary material associated with this article can be found, in the online version, at doi:10.1016/j.geothermics.2022.102378.

References

Adimalla, N., Venkatayogi, S., 2018. Geochemical characterization and evaluation of groundwater suitability for domestic and agricultural utility in semi-arid region of Basara, Telangana State, South India. Appl. Water Sci. 8 (1), 1–14.
Aggett, J., Aspell, A.C., 1978. Release of Arsenic from Geothermal Sources. New Zealand Energy Research and Development Committee.
Agusa, T., Kunito, T., Fujihara, J., Kubota, R., Minh, T.B., Trang, P.T.K., Iwata, H., Subramanian, A., Viet, P.H., Tanabe, S., 2006. Contamination by arsenic and other trace elements in tube-well water and its risk assessment to humans in Hanoi, Vietnam. Environ. Pollut. 139 (1), 95–106.
Aksoy, N., Şimşek, C., Gunduz, O., 2009. Groundwater contamination mechanism in a geothermal field: a case study of Balcova, Turkey. J. Contam. Hydrol. 103 (1–2), 13–28.
Alidadi, H., Sany, S.B.T., Oftadeh, B.Z.G., Mohamad, T., Shamszade, H., Fakhari, M., 2019. Health risk assessments of arsenic and toxic heavy metal exposure in drinking water in northeast Iran. Environ. Health Prev. Med. 24 (1), 1–17.
Angelone, M., Cremisini, C., Piscopo, V., Proposito, M., Spaziani, F., 2009. Influence of hydrostratigraphy and structural setting on the arsenic occurrence in groundwater of the Cimino-Vico volcanic area (central Italy). Hydrogeol. J. 17 (4), 901–914.
Bhattacharya, P., Claesson, M., Bundschuh, J., Sracek, O., Fagerberg, J., Jacks, G., Martin, R.A., Storniolo, A.D.R., Thir, J.M., 2006. Distribution and mobility of arsenic in the Rio Dulce alluvial aquifers in sanTiago del estero province, Argentina. Sci. Total Environ. 358 (1–3), 97–120.
Birkle, P., Merkel, B., 2000. Environmental impact by spill of geothermal fluids at the geothermal field of Los Azufres, Michoacán, Mexico. Water Air Soil Pollut. 124 (3), 371–410.
Birkle, P., Bundschuh, J., Sracek, O., 2010. Mechanisms of arsenic enrichment in geothermal and petroleum reservoirs fluids in Mexico. Water Res. 44 (19), 5605–5617.
Bischoff, J.L., Seyfried, W.E., 1978. Hydrothermal chemistry of seawater from 25 degrees to 350 °C. Am. J. Sci. 278 (6), 838–860.
Boyle, R.W., Jonasson, I.R., 1973. The geochemistry of As and its use as an indicator element in geochemical prospecting. J. Geochem. Explor. 2, 251–256.
Brown, K.L., Simmons, S.F., 2003. Precious metals in high-temperature geothermal systems in New Zealand. Geothermics 32, 619–625.
Camacho, L.M., Gutiérrez, M., Alarcón-Herrera, M.T., de Lourdes Villalba, M., Deng, S., 2011. Occurrence and treatment of arsenic in groundwater and soil in northern Mexico and southwestern USA. Chemosphere 83, 211–225.
Conrad, G., Montigny, R., Thuizat, R., Westphal, M., 1981. Tertiary and Quaternary geodynamics of southern Lut (Iran) as deduced from palaeomagnetic, isotopic and structural data. Tectonophysics 75 (3–4), T11–T17.
Deshaee, A., Shakeri, A., Taran, Y., Mehrabi, B., Farhadian, M., Zelenski, M., Chaplygin, I., Tassi, F., 2020. Geochemistry of Bazman thermal springs, southeast Iran. J. Volcanol. Geotherm. Res. 390, 106676.
Deutsch, W.J., 1997. Groundwater Geochemistry: Fundamentals and Application to Contamination. Lewis Publisher, USA.
Drever, J.I., 1988. The Geochemistry of Natural Waters, 2nd edn. Prentice-Hall, New York.
Elango, L., Kannan, R., Senthil Kumar, M., 2003. Major ion chemistry and identification ofhydrogeochemical processes of groundwater in a part of Kancheepuram district, TamilNadu, India. Environ. Geosci. 10 (4), 157–166.
Ellis, A.J., 1971. Magnesium ion concentrations in the presence of magnesium chlorite, calcite, carbon dioxide, quartz. Am. J. Sci.;(United States) 271 (5).
Feng, T., Lin, H., Guo, Q., Feng, Y., 2014. Influence of an arsenate-reducing and polycyclic aromatic hydrocarbons-degrading Pseudomonas isolate on growth and arsenic accumulation in Pteris vittata L. and removal of phenanthrene. Int. Biodeterior. Biodegradat. 94, 12–18.
Gaillardet, J., Dupré, B., Louvat, P., Allegre, C.J., 1999. Global silicate weathering and CO2 consumption rates deduced from the chemistry of large rivers. Chem. Geol. 159 (1–4), 3–30.
Garrels, R.M., 1967. Genesis of some ground waters from igneous rocks. Geochemistry 2, 405–420.
Gemici, Ü., Tarcan, G., 2002. Hydrogeochemistry of the Simav geothermal field, western Anatolia, Turkey. J. Volcanol. Geotherm. Res. 116 (3–4), 215–233.
Ghoreyshinia, S.K., Shakeri, A., Mehrabi, B., Tassi, F., Mehr, M.R., Deshaee, A., 2020. Hydrogeochemistry, circulation path and arsenic distribution in Tahlab aquifer, East of Taftan Volcano, SE Iran. Appl. Geochem. 119, 104629.
Gibbs, R.J., 1970. Mechanisms controlling world's water chemistry. Science 170, 1088–1090.
Giménez-Forcada, E., Smedley, P.L., 2014. Geological factors controlling occurrence and distribution of arsenic in groundwaters from the southern margin of the Duero Basin. Spain. Environ. Geochem. Health 36 (6), 1029–1047 https://doi.org/101007/s10653-014-9599-2.
González, E.P., Tello, E.H., Verma, M.P., 2001. Interaction between geothermal water and springs at the Los Humeros geothemal field, Puebla, Mexico. Ing. Hidraul. Mex 15 (2), 185–194.
Henke, K.R., 2009. Environmental chemistry, Health Threats and Waste Treatment. John Wiley & Sons: West Sussex, United Kingdom.
Hopenhayn-Rich, C., Biggs, M.L., Smith, A.H., 1998. Lung and kidney cancer mortality associated with arsenic in drinking water in Cordoba, Argentina. Int. J. Epidemiol. 27 (4), 561–569.
Hopenhayn-Rich, C., Biggs, M.L., Fuchs, A., Bergoglio, R., Tello, E.E., Nicolli, H., Smith, A.H., 1996. Bladder cancer mortality associated with arsenic in drinking water in Argentina. Epidemiology 117–124.
Kaasalainen, H., Stefánsson, A., 2012. The chemistry of trace elements in surface geothermal waters and steam, Iceland. Chem. Geol. 330, 60–85.
Kalantary, N., Rahimi, M., Charchi, A., 2007. Use of composite diagram, factor analyses and saturation index for quantification of Zaviercherry and Kheran plain groundwaters. J. Eng. Geol. 2 (1), 339–356.
Karizaki, V.M., 2017. Iranian dates and ethnic date-based products. J. Ethnic Foods 4 (3), 204–209.
Keller, N.S., Stefánsson, A., Sigfússon, B., 2014. Arsenic speciation in natural sulfidic geothermal waters. Geochim. Cosmochim. Acta 142, 15–26.
Kim, M.J., Nriagu, J., Haack, S., 2003. Arsenic behaviour in newly drilled wells. Chemosphere 52, 623–633.
Koffi, K.V., Obuobie, E., Banning, A., Wohnlich, S., 2017. Hydrochemical characteristics of groundwater and surface water for domestic and irrigation purposes in Vea catchment, Northern Ghana. Environ. Earth Sci. 76 (4), 185.
Komatina, M., 2004. Medical Geology: Effects of Geological Environments On Human Health. Elsevier.
Landrum, J.T., Bennett, P.C., Engel, A.S., Alsina, M.A., Pastén, P.A., Milliken, K., 2009. Partitioning geochemistry of arsenic and antimony, El Tatio geyser field, Chile. Appl. Geochem. 24 (4), 664–676.
Li, P., Wu, J., Qian, H., 2016. Hydrochemical appraisal of groundwater quality for drinking and irrigation purposes and the major influencing factors: a case study in and around Hua County, China. Arabian J. Geosci. 9 (1), 15.
López, D.L., Bundschuh, J., Birkle, P., Armienta, M.A., Cumbal, L., Sracek, O., Cornejo, L., Ormachea, M., 2012. Arsenic in volcanic geothermal fluids of Latin America. Sci. Total Environ. 429, 57–75.
Loughnan, F.C., 1969. Chemical weathering of the silicate minerals (No. 549.6 L6).
Maizel, D., Blum, J.S., Ferrero, M.A., Utturkar, S.M., Brown, S.D., Rosen, B.P., Oremland, R.S., 2016. Characterization of the extremely arsenic-resistant Brevibacterium linens strain AE038-8 isolated from contaminated groundwater in Tucumán, Argentina. Int. Biodeterior. Biodegradat. 107, 147–153.
Mladenov, N., Wolski, P., Hettiarachchi, G.M., Murray-Hudson, M., Enriquez, H., Damaraju, S., Galkaduwa, M.B., McKnight, D.M., Masamba, W., 2014. Abiotic and biotic factors influencing the mobility of arsenic in groundwater of a through-flow island in the Okavango Delta, Botswana. J. Hydrol. (Amst.) 518, 326–341.
Mohammadi, Z., Claes, H., Cappuyns, V., Nematollahi, M.J., Helser, J., Amjadian, K., Swennen, R., 2021. High geogenic arsenic concentrations in travertines and their spring waters: assessment of the leachability and estimation of ecological and health risks. J. Hazard. Mater. 409, 124429.
Mosaferi, M., Yunesian, M., Mesdaghinia, A., Nadim, A., Nasseri, S., Mahvi, A.H., 2003. Arsenic occurrence in drinking water of IR of Iran: the case of Kurdistan Province. In: Proceedings of BUET-UNU International Symposium–Fate of Arsenic in the Environment. Dhaka, Bangladesh.

Mroczek, E.K., 2005. Contributions of arsenic and chloride from the Kawerau geothermal field to the Tarawera River, New Zealand. Geothermics 34 (2), 218–233.
Mukherjee, A., Fryar, A.E., 2008. Deeper groundwater chemistry and geochemical modeling of the arsenic affected western Bengal basin, West Bengal, India. Appl. Geochem. 23 (4), 863–894.
Mukherjee, A., Fryar, A.E., O'Shea, B.M., 2009. Major Occurrences of Elevated Arsenic in Groundwater and Other Natural Waters. Arsenic: Environmental chemistry, health threats and waste treatment, pp. 303–350.
Mukherjee, A., Scanlon, B.R., Fryar, A.E., Saha, D., Ghosh, A., Chowdhuri, S., Mishra, R., 2012. Solute chemistry and arsenic fate in aquifers between the Himalayan foothills and Indian craton (including central Gangetic plain): influence of geology and geomorphology. Geochim. Cosmochim. Acta 90, 283–302.
Narsimha, A., Sudarshan, V., 2017. Assessment of fluoride contamination in groundwater from Basara, Adilabad district, Telangana state, India. Appl. Water Sci. 7 (6), 2717–2725.
Nickson, R.T., McArthur, J.M., Shrestha, B., Kyaw-Myint, T.O., Lowry, D., 2005. Arsenic and other drinking water quality issues, Muzaffargarh District, Pakistan. Appl. Geochem. 20 (1), 55–68.
Nimick, D.A., Moore, J.N., Dalby, C.E., Savka, M.W., 1998. The fate of geothermal arsenic in theMadison and Missouri Rivers, Montana and Wyoming. Water Resour. Res. 34 (11), 3051–3067.
Pal, T., Mukherjee, P.K., Sengupta, S., Bhattacharyya, A.K., Shome, S., 2002. Arsenic pollution in groundwater of West Bengal, India-an insight into the problem by subsurface sediment analysis. Gondwana Res. 5 (2), 501–512.
Pang, K.N., Chung, S.L., Zarrinkoub, M.H., Chiu, H.Y., Li, X.H., 2014. On the magmatic record of the Makran arc, southeastern Iran: insights from zircon U-Pb geochronology and bulk-rock geochemistry. Geochem. Geophys. Geosyst. 15 (6), 2151–2169.
Parkhurst, D.L., Appelo, C.A.J., 1999. User's Guide to PHREEQC (Version 2) – A Computer Program for Speciation, Batch-Reaction, One-Dimensional Transport, and Inverse Geochemical Calculations. United States Geological Survey, Water Resources Investigations Report 99-4259, Washington, DC, p. 326.
Planer-Friedrich, B., London, J., McCleskey, R.B., Nordstrom, K.D., Wallschlager, D., 2007. Thioarsenates in geothermal waters of Yellowstone National Park: determination, preservation, and geochemical importance. Environ. Sci. Technol. 41, 5245–5251.
Rastegari Mehr, M., Keshavarzi, B., Moore, F., Hooda, P.S., Busquets, R., Ghorbani, Z., 2020. Arsenic in the rock–soil–plant system and related health risk in a magmatic–metamorphic belt, West of Iran. Environ. Geochem. Health 42, 3659–3673.
Rielel, F.N., Eikman, T., 1986. Natural occurrences of arsenic and its compounds in soils and rocks. Wiss. Umw 3–4, 108–117.
Robinson, B., Duwig, C., Bolan, N., Kannathasan, M., Saravanan, A., 2003. Uptake of arsenic by New Zealand watercress (Lepidium sativum). Sci. Total Environ. 301 (1–3), 67–73.
Rodríguez-Lado, L., Sun, G., Berg, M., Zhang, Q., Xue, H., Zheng, Q., Johnson, C.A., 2013. Groundwater arsenic contamination throughout China. Science 341 (6148), 866–868.
Rose, A.W., Hawkas, H.E., Webb, J.S., 1979. Geochemistry in Mineral Exploration. Academic Press, London.
Saadat, S., Stern, C.R., 2011. Petrochemistry and genesis of olivine basalts from small monogenetic parasitic cones of Bazman stratovolcano, Makran arc, southeastern Iran. Lithos 125 (1–2), 607–619.
Sahandi, M.R., Padashi, M., 2005. Geological Quadrangle Map of Iran (1:100000 Scale), Sheet 8045 (Bazman). Geology Survey, Tehran, Iran.
Schwenzer, S.P., Tommaseo, C.E., Kersten, M., Kirnbauer, T., 2001. Speciation and oxidation kinetics of arsenic in the thermal springs of Wiesbaden spa, Germany. Fresenius J. Anal. Chem. 371, 927–933.
Shah, A.A., Nawaz, A., Kanwal, L., Hasan, F., Khan, S., Badshah, M., 2015. Degradation of poly (ε-caprolactone) by a thermophilic bacterium Ralstonia sp. strain MRL-TL isolated from hot spring. Int. Biodeterior. Biodegradat. 98, 35–42.
Shakeri, A., Fard, M.S., Mehrabi, B., Mehr, M.R., 2020. Occurrence, origin and health risk of arsenic and potentially toxic elements (PTEs) in sediments and fish tissues from the geothermal area of the Khiav River, Ardebil Province (NW Iran). J. Geochem. Explor 208, 106347.
Shakeri, A., Ghoreyshinia, S., Mehrabi, B., Delavari, M., 2015. Rare earth elements geochemistry in springs from Taftan geothermal area SE Iran. J. Volcanol. Geotherm. Res. 304, 49–61.
Shamsudduha, M., Uddin, A., Saunders, J.A., Lee, M.K., 2008. Quaternary stratigraphy, sediment characteristics and geochemistry of arseniccontaminated alluvial aquifers in the Ganges–Brahmaputra floodplain in central Bangladesh. J. Contam. Hydrol. 99, 112–136. https://doi.org/10.1016/j.jconhyd.2008.03.010 (this issue).
Sharifi, R., Moore, F., Keshavarzi, B., 2016. Mobility and chemical fate of arsenic and antimony in water and sediments of Sarouq River catchment, Takab geothermal field, northwest Iran. J. Environ. Manage. 170, 136–144.
Sheikhi, S., Faraji, Z., Aslani, H., 2021. Arsenic health risk assessment and the evaluation of groundwater quality using GWQI and multivariate statistical analysis in rural areas, Hashtroud, Iran. Environ. Sci. Pollut. Res. 28 (3), 3617–3631.
Smedley, P.L., Kinniburgh, D.G., 2002. A review of the source, behaviour and distribution of arsenic in natural waters. Appl. Geochem. 17 (5), 517–568.
Smedley, P.L., Nicolli, H.B., Macdonald, D.M.J., Barros, A.J., Tullio, J.O., 2002. Hydrogeochemistry of arsenic and other inorganic constituents in groundwaters from La Pampa, Argentina. Appl. Geochem. 17 (3), 259–284.
Smith, A.H., Goycolea, M., Haque, R., Biggs, M.L., 1998. Marked increase in bladder and lung cancer mortality in a region of Northern Chile due to arsenic in drinking water. Am. J. Epidemiol. 147 (7), 660–669.
Song, Q., Zeng, X., Li, J., Duan, H., Yuan, W., 2015. Environmental risk assessment of CRT and PCB workshops in a mobile e-waste recycling plant. Environ. Sci. Pollut. Res. 22 (16), 12366–12373.
Srinivasamoorthy, K., Chidambaram, S., Prasanna, M.V., Vasanthavihar, M., Peter, J., Anandhan, P., 2008. Identification of major sources controlling groundwater chemistry from a hard rock terrain—A case study from Mettur taluk, Salem district, Tamil Nadu, India. J. Earth Syst. Sci. 117 (1), 49.
Tardy, Y., 1971. Characterization of the principal weathering types by the geochemistry of waters from some European and African crystalline massifs. Chem. Geol. 7, 253–271.
Tseng, C.H., Chong, C.K., Tseng, C.P., Hsueh, Y.M., Chiou, H.Y., Tseng, C.C., Chen, C.J., 2003. Long-term arsenic exposure and ischemic heart disease in arseniasis-hyperendemic villages in Taiwan. Toxicol. Lett. 137 (1–2), 15–21.
USEPA (United States Environmental Protection Agency), 2011. USEPA regional screening Level (RSL) summary table: November 2011. Available at. http://www.epa.gov/regshwmd/risk/human/Index.htm.
Vahdati Daneshmand, F., Berberian, M., Jorjandi, M., 2004. Geological Quadrangle Map of Iran (1:100000 Scale), Sheet 7945 (Maksan). Geology Survey, Tehran: Iran.
Waheed, S., Siddique, N., Rahman, A., Saeed, S., Zaidi, J.H., Ahmad, S., 2005. INAA and ETAAS of toxic element content of fruits harvested and consumed in Pakistan. J. Radioanal. Nucl. Chem. 262 (3), 691–696.
Webster, J.G., Nordstrom, D.K., 2003. Geothermal arsenic. Arsenic in Ground Water. Springer, Boston, MA, pp. 101–125.
WHO, 2011. Guidelines for Drinking-Water Quality, 4rd ed, 1. world Health organization, Geneva, Switzerland, p. 564.
Wilkie, J.A., Hering, J.G., 1998. Rapid oxidation of geothermal arsenic (III) in streamwaters of the eastern Sierra Nevada. Environ. Sci. Technol. 32 (5), 657–662.
Zaidi, F.K., Nazzal, Y., Jafri, M.K., Naeem, M., Ahmed, I., 2015. Reverse ion exchange as a major process controlling the groundwater chemistry in an arid environment: a case study from northwestern Saudi Arabia. Environ. Monit. Assess 187 (10), 1–18.
Zartarian, V.G., Xue, J., Özkaynak, H., Dang, W., Glen, G., Smith, L., Stallings, C., 2006. A probabilistic arsenic exposure assessment for children who contact CCA-treated playsets and decks, Part 1: model methodology, variability results, and model evaluation. Risk Anal. 26 (2), 515–531.
Zhang, Q., Rodríguez-Lado, L., Johnson, C.A., Xue, H., Shi, J., Zheng, Q., Sun, G., 2012. Predicting the risk of arsenic contaminated groundwater in Shanxi Province, Northern China. Environ. Pollut. 165, 118–123.